

Red Supergiant Stars within the Local Group

Lee. R. Patrick



Doctor of Philosophy
The University of Edinburgh
March 2016

Chapter 1

First steps outside the Local Group of Galaxies: Red Supergiants in NGC 55

1.1 Opening remarks

Owen has kindly helped reconstruct and combine the data sets

1.2 Introduction

NGC 55 is a galaxy located outside of the Local Group of Galaxies potentially within the Sculptor Group at a distance of 1.94 ± 0.03 Mpc (Pietrzyński et al., 2006; Gieren et al., 2008) which, before the emergence of the Araucaria Project (Gieren et al., 2005), been subject to considerable uncertainty (Pritchett et al., 1987; van de Steene et al., 2006, e.g.).

The Sculptor Group is considered to be the closest group of galaxies to our own and offers a fantastic laboratory with which to test theories of stellar and galactic evolution. Association to the Sculptor group however, is a contentious issue. Distance estimates vary to each galaxy, but typically when one references this group the main galaxies associated to this reference are: NGC 55, NGC 247, NGC 253, NGC 300 and NGC 7793. In addition to these five large spiral galaxies,



Figure 1.1 *Image of NGC 55 from the Wide Field Imager on the 2.2-metre MPG/ESO telescope at ESO La Silla Observatory. Credit: ESO Should go the whole hog and bootstrap the RSGs and footprints onto this image ...*

there are also numerous (~ 20) dwarf galaxies associated to this group.

By revising distances for nine of these dwarfs Karachentsev et al. (2003) postulated that the Sculptor group was actually more like a filament of galaxies, which intersects the Milky Way group, where NGC 55 and NGC 300 and their surrounding satellite galaxies were potentially not associated with the main group of galaxies in this filament. Regardless of the geometry and association to the Sculptor Group, NGC 55 is the nearest large galaxy to the MW group in the direction of the Sculptor Group.

The morphology of NGC 55 is asymmetric and complicated owing to the high inclination angle measured for this galaxy (up to 80° ; Hummel, Dettmar & Wielebinski, 1986; Westmeier, Koribalski & Braun, 2013). de Vaucouleurs (1961) classified this galaxy as an LMC-like spiral barred galaxy (SB(s)m) prompting some claims that this galaxy is an edge on analogue of the LMC. Figure 1.3 shows NGC 55 and its complicated morphology. In addition, NGC 55

NGC 55 and NGC 300 are clearly associated, given their locations on the sky and distance estimates This nearest neighbour galaxy group contains five spiral galaxies (NGC 55, NGC 300)

- What is NGC 55?
- Why is it important?
- What other studies of abundances are present in NGC 55
- Any controversies? e.g. its distance, association to Sculptor group etc.

1.3 Observations

The observations for this study were taken using three nights of KMOS guaranteed time observations (GTO) containing xx RSG candidates, the first of which was taken in October 2013 as part of the observations which led to the publication of Gazak et al. (2015). These data consisted of six science exposures (S) of 600s with sky offset exposures (S) interleaved in an O, S, O observing pattern. Seeing conditions for these data were good at $0''.8$ – $1''.2$ throughout the course of the observing block (OB).

The second data set which is made use of in this chapter comes from two nights in September 2014 where the OB used in 2013 was used as backup observations for a programme which required excellent seeing ($<0''.6$). The seeing limits on our observations are more relaxed ($<1''.5$) which gave us an opportunity to make use of some slightly poorer quality KMOS data. On the first night in September 2014 where this OB was observed, the seeing conditions varied widely ($>1''.6$) prompting one observer to comment that “this is the worst recorded seeing at Paranal!”. However, there are 24 science exposures where the seeing conditions were better than $2''.2$, which are (potentially) useful. The final night of observing consisted of 12 exposures with seeing conditions varying between $1''.1$ – $1''.6$.

In addition to the science exposures obtained, on each night a standard set of KMOS calibration files were obtained as well as standard star observations on each night. The standard star observing block for each night is slightly different where in October 2013 HIP 3820 (Houk, 1978, B8 V;) was observed using the 24-arm telluric template (KMOS_spec_acq_stdstarscipatt). However, in September 2014 only the three-arm telluric template was observed (KMOS_spec_cal_stdstar), this time with HIP 18926 (Houk & Smith-Moore, 1988, B3 V;) and HIP 3820 on both nights.

interestingly both with radial velocity measurements. Could do

Table 1.1 Measured velocity resolution and resolving power across each detector.

Date	Det.	IFUs	Ne $\lambda 1.17700 \mu\text{m}$		Ar $\lambda 1.21430 \mu\text{m}$	
			FWHM (km s $^{-1}$)	R	FWHM (km s $^{-1}$)	R
16-10-2013	1	1-8	95.48 \pm 2.46	3140 \pm 81	90.78 \pm 2.12	3302 \pm 77
	2	9-16	88.91 \pm 1.66	3371 \pm 63	86.30 \pm 1.85	3473 \pm 74
	3	17-24	82.96 \pm 2.14	3612 \pm 76	80.77 \pm 2.14	3712 \pm 98
14-09-2015	1	1-8	84.18 \pm 1.93	3561 \pm 82	90.78 \pm 2.12	3302 \pm 77
	2	9-16	87.00 \pm 1.69	3446 \pm 67	84.67 \pm 1.93	3541 \pm 81
	3	17-24	97.14 \pm 1.88	3086 \pm 60	94.85 \pm 2.01	3161 \pm 67
15-09-2014	1	1-8	82.55 \pm 1.96	3632 \pm 86	80.41 \pm 2.30	3728 \pm 106
	2	9-16	88.08 \pm 1.78	3404 \pm 69	86.03 \pm 1.96	3485 \pm 80
	3	17-24	98.04 \pm 1.91	3058 \pm 59	96.74 \pm 2.05	3099 \pm 66

some nice calibration of the RV measurements? or update their measurements ... remember, we've chosen them to be featureless in this region

Table 1.1 shows the mean measured resolution and resolving power, at the appropriate rotator angles, for each night where the NGC 55 data were taken. This table shows that the resolution can vary significantly between each night, particularly on detector three where the mean resolving power changes by a factor of 1/5.

1.3.1 Target Selection

Targets were selected based on the optical photometry from the Araucaria Project (Gieren et al., 2005). The optical CMD which is used to select targets is displayed in Figure 1.2, where the RSG candidates are within the grey box and the observed targets are highlighted in red. This method of target selection was chosen based on the limited extent of near-IR photometry in this area. Figure 1.3 displays the footprints from the Araucaria Project (green) and the ACS Nearby Galaxy Survey Treasury (blue; ANGST Dalcanton et al., 2009) in NGC 55 overlaid on a — image.

The selection criteria employed in this study makes use of the optical $V - I$ colours and m_I magnitudes. Owing to their cool temperatures and extreme luminosities RSGs are known to exist in a “plume” at the tip of a structure of cool stars in the

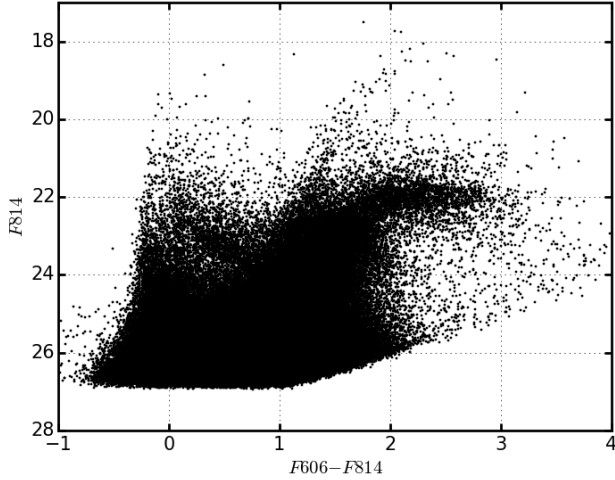


Figure 1.2 Colour magnitude diagram for the NGC 55 optical photometry from the Araucaria Project Gieren et al. (2005). *placeholder! – currently this is from the ANGST data*

$V - I, m_I$ CMD (?) Figure 1.2 displays this CMD and the region of parameter space where RSG candidates reside is marked with a grey box. This box has the limits $17 < m_I < 19$ and $1.2 < V - I < 3.5$ following Gazak et al. (2015). The lower limit of this box are naturally blended in to a population of super-AGB stars which can have luminosities comparable to the faintest RSGs (Nikolaev & Weinberg, 2000, e.g.). However, as stated in Chapter ?? these stars are known to have lifetimes similar to the lowest mass RSGs and arguably still trace the young stellar population of this galaxy.

Table 1.2 shows ground- and space-based optical photometry of the KMOS targets along with their radial velocities (see section 1.5.1).

1.4 Data Reduction

The data reduction was performed with the KMOS/esorex pipeline with a several corrections to improve the quality of the reductions which are fully described and characterised in ?.

- Split recombined sky frames into seeing bins
- combine by including pixel shifts between reconstructed IFUs to ensure all frames are correctly matched

Table 1.2 Summary of *VLT-KMOS* targets in *NGC 55*.

ID	S/N	α (J2000)	δ (J2000)	V	I	F606	F814	r^o	(km s $^{-1}$)	Notes
									15-09-2014	
NGC55-RSG19	xx	00:15:29.190	-39:14:08.20	V	17.73	F606	F814	RV1	RV2	RV3
NGC55-RSG20	xx	00:15:29.520	-39:15:13.00	V	18.95	F606	F814	RV1	RV2	RV3
NGC55-RSG22	xx	00:15:30.520	-39:16:36.70	V	18.56	F606	F814	RV1	RV2	RV3
NGC55-RSG24	xx	00:15:31.460	-39:14:46.30	V	18.48	F606	F814	RV1	RV2	RV3
NGC55-RSG25	xx	00:15:31.490	-39:14:32.40	V	18.39	F606	F814	RV1	RV2	RV3
NGC55-RSG26	xx	00:15:33.160	-39:13:42.00	V	17.96	F606	F814	RV1	RV2	RV3
NGC55-RSG28	xx	00:15:36.160	-39:15:29.40	V	18.99	F606	F814	RV1	RV2	RV3
NGC55-RSG30	xx	00:15:38.030	-39:14:50.20	V	18.73	F606	F814	RV1	RV2	RV3
NGC55-RSG35	xx	00:15:39.260	-39:15:01.70	V	17.87	F606	F814	RV1	RV2	RV3
NGC55-RSG36	xx	00:15:39.520	-39:16:23.10	V	18.46	F606	F814	RV1	RV2	RV3
NGC55-RSG39	xx	00:15:40.260	-39:15:01.00	V	17.97	F606	F814	RV1	RV2	RV3
NGC55-RSG43	xx	00:15:40.700	-39:14:50.20	V	18.18	F606	F814	RV1	RV2	RV3
NGC55-RSG46	xx	00:15:41.640	-39:14:58.80	V	18.44	F606	F814	RV1	RV2	RV3
NGC55-RSG57	xx	00:15:45.590	-39:15:16.40	V	18.22	F606	F814	RV1	RV2	RV3
NGC55-RSG58	xx	00:15:46.270	-39:15:43.20	V	18.40	F606	F814	RV1	RV2	RV3
NGC55-RSG60	xx	00:15:49.180	-39:17:19.80	V	18.85	F606	F814	RV1	RV2	RV3
NGC55-RSG65	xx	00:15:51.250	-39:16:26.40	V	17.65	F606	F814	RV1	RV2	RV3
NGC55-RSG67	xx	00:15:53.110	-39:14:13.60	V	18.05	F606	F814	RV1	RV2	RV3
NGC55-RSG69	xx	00:15:55.280	-39:15:00.10	V	18.67	F606	F814	RV1	RV2	RV3
NGC55-RSG70	xx	00:15:56.310	-39:16:08.60	V	18.91	F606	F814	RV1	RV2	RV3
NGC55-RSG71	xx	00:15:56.900	-39:15:27.50	V	18.56	F606	F814	RV1	RV2	RV3
NGC55-RSG73	xx	00:15:57.710	-39:15:41.50	V	18.41	F606	F814	RV1	RV2	RV3

Ground based data from the Araucaria Project Pietrzynski et al. (2006), with typical photometric uncertainty 0.01 and 0.01 in V and I bands respectively. Supplementary ANGST data from Dalcanton et al. (2009), with typical errors 0.015, 0.010, 0.012, in J, H and K bands respectively.

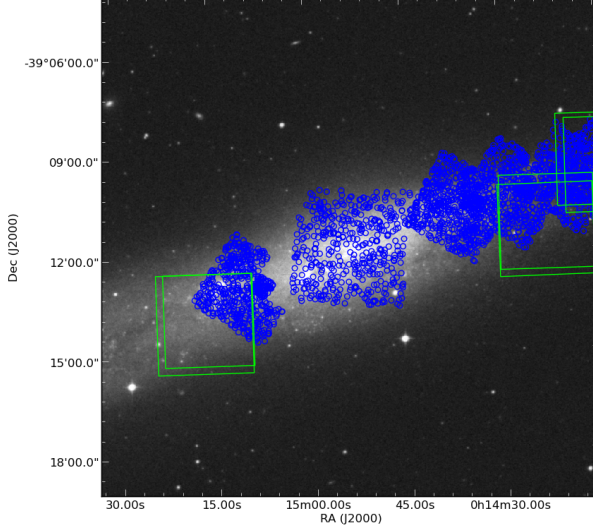


Figure 1.3 Image of NGC 55 with KMOS targets overlaid in red and photometric footprints from the Araucaria Project (Gieren et al., 2005) and the ANGST project (Dalcanton et al., 2009) highlighted with black shapes. *placeholder! Should do this properly and overlay the regions etc on the pretty eso image.*

- etc.

Would it be useful to use Skycorr to subtract the sky as in Gazak et al. (2015)

Telluric correction has been performed by combining and reconstrucitng the telluric standard exposures using the standard pipeline routines. To improve the performance of the telluric correction I use the method described in detail in Chapter ??.

As mentioned above, were multiple standard star OBs for each night of observing. The telluric spectrum used to correct each science spectrum is determined on a star-by-star basis depending upon a visual inspection of the results of the correction.

1.5 Results

1.5.1 Radial Velocities

- Association with NGC 55
- Does this deserve a subsection of its own?
- Radial velocity Vs. Radius from galaxy centre

1.5.2 Stellar Parameters

- Comparison to previous results
- Z Vs. Radius from galaxy centre
- MCMC parameter estimation for the fit

1.6 Discussion

- Orientation of NGC 55

1.7 Conclusions

Bibliography

- Dalcanton J. J. et al., 2009, ApJS, 183, 67
- de Vaucouleurs G., 1961, ApJ, 133, 405
- Gazak J. Z. et al., 2015, ApJ, 805, 182
- Gieren W. et al., 2005, The Messenger, 121, 23
- Gieren W., Pietrzyński G., Soszyński I., Bresolin F., Kudritzki R.-P., Storm J., Minniti D., 2008, ApJ, 672, 266
- Houk N., 1978, Michigan catalogue of two-dimensional spectral types for the HD stars
- Houk N., Smith-Moore M., 1988, Michigan Catalogue of Two-dimensional Spectral Types for the HD Stars. Volume 4, Declinations -26deg .0to – 12deg.0.
- Hummel E., Dettmar R.-J., Wielebinski R., 1986, A&A, 166, 97
- Karachentsev I. D. et al., 2003, A&A, 404, 93
- Nikolaev S., Weinberg M. D., 2000, ApJ, 542, 804
- Pietrzyński G. et al., 2006, AJ, 132, 2556
- Pritchett C. J., Schade D., Richer H. B., Crabtree D., Yee H. K. C., 1987, ApJ, 323, 79
- van de Steene G. C., Jacoby G. H., Praet C., Ciardullo R., Dejonghe H., 2006, A&A, 455, 891
- Westmeier T., Koribalski B. S., Braun R., 2013, MNRAS, 434, 3511